Phosphorylation of the RNA-binding protein Dazl by MAPKAP kinase 2 regulates spermatogenesis

Patrick A. Williams, Michael S. Krug, Emily A. McMillan, Jasmine D. Peake, Tara L. Davis, Simon Cocklin, and Todd I. Strochlic*
Department of Biochemistry and Molecular Biology, Drexel University College of Medicine, Philadelphia, PA 19102

ABSTRACT **Developing male germ cells are exquisitely sensitive to environmental insults such as heat and oxidative stress. An additional characteristic of these cells is their unique dependence on RNA-binding proteins for regulating posttranscriptional gene expression and translational control. Here we provide a mechanistic link unifying these two features. We show that the germ cell–specific RNA-binding protein deleted in azoospermia-like (Dazl) is phosphorylated by MAPKAP kinase 2 (MK2), a stress-induced protein kinase activated downstream of p38 MAPK. We demonstrate that phosphorylation of Dazl by MK2 on an evolutionarily conserved serine residue inhibits its interaction with poly(A)-binding protein, resulting in reduced translation of Dazl-regulated target RNAs. We further show that transgenic expression of wild-type human Dazl but not a phosphomimetic form in the *Drosophila* male germline can restore fertility to flies deficient in *boule*, the *Drosophila* orthologue of human Dazl. These results illuminate a novel role for MK2 in spermatogenesis, expand the repertoire of RNA-binding proteins phosphorylated by this kinase, and suggest that signaling by the p38-MK2 pathway is a negative regulator of spermatogenesis via phosphorylation of Dazl.**

Monitoring Editor
Julie Brill
The Hospital for Sick Children

Received: Nov 13, 2015
Revised: May 24, 2016
Accepted: Jun 3, 2016

INTRODUCTION

Spermatogenesis is a highly coordinated process during which developing male germ cells experience periods of transcriptional quiescence despite a requirement for continued protein synthesis (Hecht, 1998). The process is therefore heavily reliant on posttranscriptional mechanisms for regulating gene expression. RNA-binding proteins fulfill this function by stabilizing presynthesized transcripts that are to be translated at later stages of spermatogenesis (Paronetto and Sette, 2010; Idler and Yan, 2012). Consequently, deletion of several RNA-binding proteins in male mice results in meiotic arrest and infertility (Venables and Cooke, 2000; Dass *et al.*, 2007; Gutti *et al.*, 2008; Hsu *et al.*, 2008), illustrating the importance of these proteins in male germ cell development. An additional property of developing male germ cells is their exquisite sensitivity to heat stress, and even mild, transient hyperthermia induces germ cell apoptosis with detrimental consequences for fertility (Yin *et al.*, 1997; Rockett *et al.*, 2001). Although the underlying molecular mechanisms that mediate these effects are not entirely understood, p38 MAP kinase plays an important role in this process (Jia *et al.*, 2009). A primary target of activated p38 is the serine/threonine kinase mitogen-activated protein kinase–activated protein kinase 2 (MK2/MAPKAPK2; Stokoe *et al.*, 1992). Direct phosphorylation of MK2 on two threonine residues (T222 and T334) results in its activation (Ben-Levy *et al.*, 1995). However, the precise role of MK2 in spermatogenesis is unknown.

Here we show that the germ cell–specific RNA-binding protein deleted in azoospermia-like (Dazl) is phosphorylated by MK2. We demonstrate that phosphorylation of Dazl by MK2 inhibits its association with poly(A)-binding protein, resulting in reduced translation of Dazl-regulated RNA targets both in vitro and in a transgenic *Drosophila* model system. These findings establish a novel connection between stress-induced kinase signaling and translational regulation by RNA-binding proteins in the male germline.

RESULTS AND DISCUSSION

Dazl is a novel substrate of MK2

To characterize a potential role for MK2 signaling in male germ cell development, we conducted a proteomic screen to identify novel substrates of this kinase. Expression of MK2 was reduced by short hairpin RNA (shRNA) in SUM149 cells, a triple-negative breast

This article was published online ahead of print in MBoC in Press (http://www.molbiolcell.org/cgi/doi/10.1091/mbc.E15-11-0773) on June 8, 2016.

*Address correspondence to: Todd I. Strochlic (Todd.Strochlic@drexelmed.edu).

Abbreviations used: Dazl, deleted in azoospermia-like; MK2/MAPKAPK2, mitogen-activated protein kinase–activated protein kinase 2; PABP, poly(A)-binding protein; RRM, RNA recognition motif.

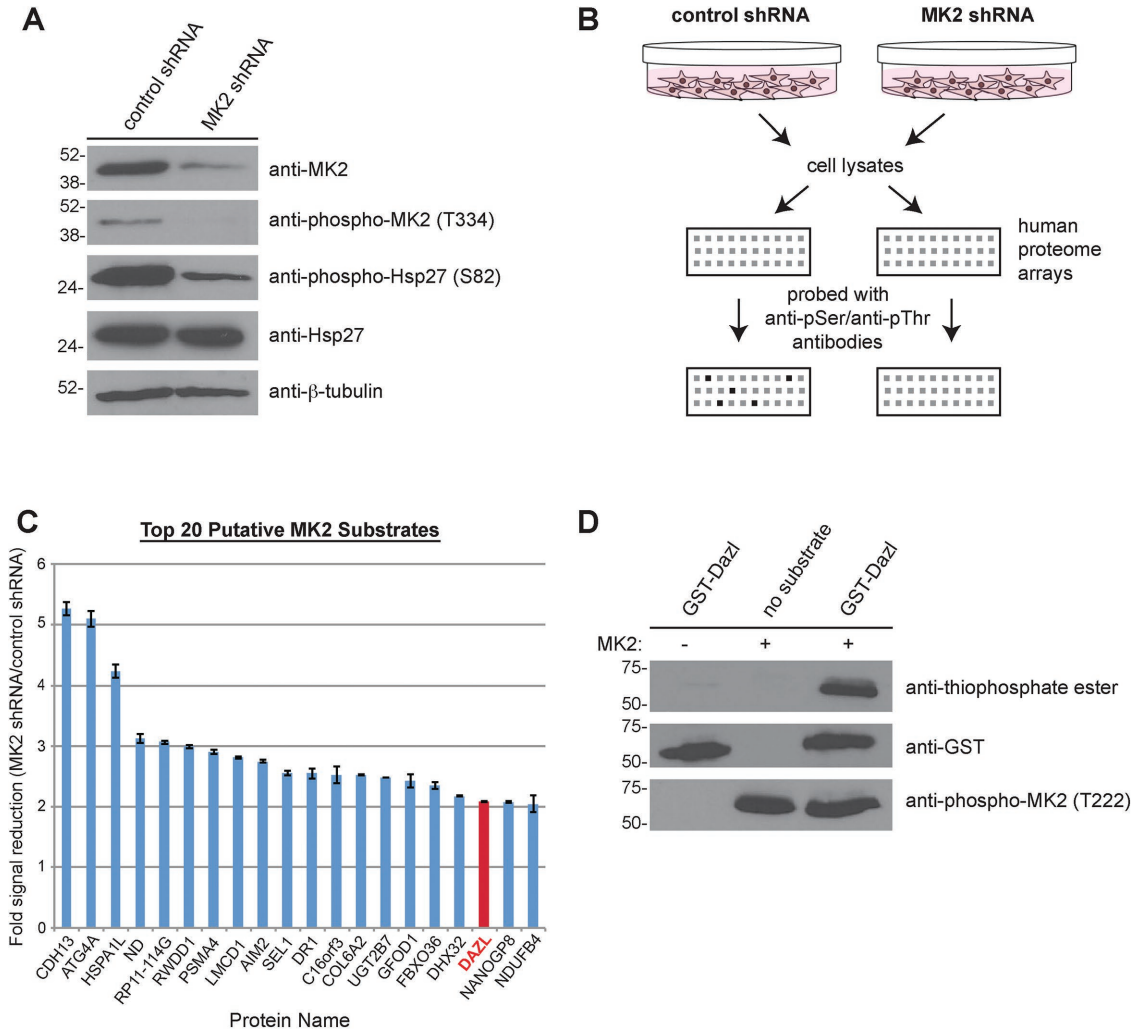

FIGURE 1: Dazl is a novel substrate of MK2. (A) Reduction of MK2 expression by shRNA. Cell lysates from SUM149 cells stably expressing either control or MK2 shRNA were resolved by SDS–PAGE (on two separate gels) and immunoblotted with the indicated antibodies. (B) Schematic of the screen used to identify novel MK2 substrates. Lysates from control and MK2 shRNA cells were incubated with human protein microarrays and probed with anti-phosphoserine and anti-phosphothreonine antibodies, followed by detection with Alexa 488–conjugated secondary antibodies. Arrays were scanned and quantified. See *Materials and Methods* for additional details. (C) Bar graph of the top 20 putative MK2 substrates identified from the screen. Data are plotted as the average fold signal reduction obtained from the MK2- knockdown shRNA array compared with the control shRNA knockdown array. Error bars indicate SD. (D) In vitro kinase assay using GST-Dazl and MK2. GST-Dazl (or no substrate) was incubated in the presence or absence of active recombinant MK2 and ATPγS, followed by treatment with PNBM. Kinase reactions were resolved by SDS–PAGE (on three separate gels), followed by immunoblotting with the indicated antibodies.

cancer cell line characterized by overexpression of catalytically active MK2 (Figure 1A). Immunoblotting of cell lysates confirmed the efficacy of MK2 knockdown compared with control shRNA–treated cells and demonstrated reduced phosphorylation of Hsp27, a known substrate of MK2 (Figure 1A). These cell lysates were applied to human proteome microarrays and incubated in the presence of ATP. Subsequent probing of these arrays with anti-phosphoserine and anti-phosphothreonine antibodies revealed differences in signal intensity between the arrays incubated with the control versus the MK2-knockdown cell lysates (Figure 1B), signifying the presence of putative MK2 substrates.

The screen for MK2-specific substrates identified 109 proteins (out of >20,000) displaying a statistically significant reduction in phosphorylation status upon MK2 knockdown (Supplemental Table S1). Among the top 20 putative MK2 substrates (Figure 1C) was deleted in azoospermia-like (Dazl), a germ cell–specific RNA-binding protein. Dazl belongs to the *DAZ* family of proteins, which also includes DAZ and Boule (Brook *et al.*, 2009). The *DAZ* family of proteins has an evolutionarily conserved role in regulating gametogenesis (Xu *et al.*, 2001; Reynolds and Cooke, 2005; Vangompel and Xu, 2011). *DAZL*-knockout male mice are sterile due to a block in meiosis (Ruggiu *et al.*, 1997; Saunders *et al.*, 2003), and men with mutations in this RNA-binding protein exhibit varying degrees of spermatogenic defects (Tung *et al.*, 2006). The fact that Dazl was identified in this screen was of particular interest, given the established function of MK2 in phosphorylating and regulating several other RNA-binding proteins in the context of inflammation (Gaestel, 2006). MK2, for instance, phosphorylates the RNA-binding proteins

tristetraprolin (Mahtani *et al.*, 2001) and hnRNP A0 (Rousseau *et al.*, 2002), ultimately resulting in the stabilization of transcripts encoding proinflammatory cytokines (Kotlyarov *et al.*, 1999; Winzen *et al.*, 1999).

To validate the screen and confirm that the RNA-binding protein Dazl is indeed a substrate of MK2, we expressed and purified human glutathione *S*-transferase (GST)–Dazl from bacteria. This fusion protein was used as a substrate in an in vitro kinase assay with active recombinant MK2. MK2 phosphorylated GST-Dazl in vitro (Figure 1D), demonstrating that Dazl is a bona fide substrate of this kinase.

MK2 phosphorylates Dazl at S65 within the RNA recognition motif

To investigate the biological role of this posttranslational modification, we determined the residue(s) on Dazl that are phosphorylated by MK2. Dazl consists of two functional domains (Figure 2A): an evolutionarily conserved RNA recognition motif (RRM), which binds target RNA sequences, and a deleted in azoospermia (DAZ) repeat important for protein–protein interactions (Brook *et al.*, 2009). The consensus motif for MK2 phosphorylation has been determined (Stokoe *et al.*, 1993), and its defining features include the presence of an arginine residue at the −3 position (i.e., three residues N-terminal to the phosphoacceptor site) and hydrophobic residues at the −5 and −6 positions. Primary sequence analysis of Dazl revealed a serine residue (S65) in the RRM located within an ideal consensus motif for MK2 phosphorylation (Figure 2A). To test whether this site was phosphorylated by MK2, we generated GST-fusion proteins of either the wild-type RRM or a mutant RRM in which this serine residue was replaced with nonphosphorylatable alanine (S65A). These fusion proteins were used as substrates in in vitro kinase reactions with active recombinant MK2 (Figure 2B). The results demonstrate that S65 is a site of MK2 phosphorylation, as mutation of this residue to alanine abolished the signal. To test whether S65 is the sole site of MK2 phosphorylation, we produced full-length GST-Dazl and GST-Dazl-S65A and used them as substrates in in vitro kinase assays. Results of this experiment reveal that mutation of this residue within the context of the full-length protein abrogated the signal, indicating that S65 is the only residue in Dazl phosphorylated by MK2 (Supplemental Figure S1). Of interest, S65 and its surrounding amino acid sequence are conserved in Dazl from zebrafish and mouse as well as in human DAZ (Xu *et al.*, 2001), and S65 phosphorylation of murine Dazl has been detected by mass spectrometry (Wu *et al.*, 2012), indicating that this posttranslational modification occurs in vivo.

To study the physiological relevance of Dazl-S65 phosphorylation, we generated a phosphospecific antibody. We first validated the specificity of this reagent by performing an in vitro kinase assay using MK2 and GST-Dazl-RRM or GST-Dazl-RRM-S65A. A signal was detected when MK2 was incubated with the wild-type Dazl-RRM but not Dazl-RRM-S65A (Figure 2C), demonstrating that the antibody detects Dazl only when phosphorylated at S65. To determine whether phosphorylation of Dazl-S65 could be detected in cells, we cotransfected HEK293 cells with constructs encoding hemagglutinin (HA)-Dazl and myc-MK2. Cells were then stimulated (or not) with sodium arsenite, a chemical that induces oxidative stress and is a potent activator of p38 MAPK. Immunoblotting of cell lysates demonstrated activation of p38 and MK2 upon stimulation and a signal using the anti–phospho-Dazl-S65 antibody (Figure 2D).

We then addressed whether genetic perturbation of the p38-MK2 signaling pathway affects phosphorylation of Dazl. HEK293 cells were transfected with plasmids encoding HA-Dazl, myc-MK2, and either a dominant-negative mutant of p38α (FLAG-p38-AF) or a constitutively active form of MK2 (myc-MK2-EE). Immunoblotting of cell lysates revealed a lack of Dazl-S65 phosphorylation in arsenite-stimulated cells expressing dominant-negative p38 (Figure 2D). However, even in the absence of stimulation, Dazl-S65 phosphorylation was detected in cells expressing constitutively active MK2 (Figure 2D). Furthermore, chemical inhibition of the p38-MK2 pathway using the p38 MAPK inhibitor SB203580 or MK2 inhibitor III confirmed that phosphorylation of Dazl-S65 was dependent on MK2 kinase activity (Figure 2E). Collectively these data indicate that serine 65 of Dazl is phosphorylated by MK2.

S65 phosphorylation of Dazl negatively regulates translation but not RNA binding

Within male germ cells, Dazl stabilizes several mRNAs that encode proteins with critical functions in meiosis, such as the synaptonemal complex component Sycp3 (Reynolds *et al.*, 2007) and the DEAD-box RNA helicase Mvh/Ddx4 (Reynolds *et al.*, 2005). As a result, deletion of *DAZL* in male mice results in reduced protein expression of Sycp3 (Reynolds *et al.*, 2007) and Mvh (Reynolds *et al.*, 2005), culminating in meiotic arrest.

Previous studies examining the RNA-binding properties of Dazl determined that the protein preferentially binds to a loosely defined uridine-rich consensus sequence in the 3′ untranslated region (UTR) of these transcripts (Venables *et al.*, 2001; Jiao *et al.*, 2002; Maegawa *et al.*, 2002). Because the MK2 phosphorylation site we identified was located within the RRM of Dazl, we speculated that modification at this site affects RNA binding. To directly test this hypothesis, we used surface plasmon resonance (SPR). Synthetic biotinylated RNA molecules consisting of the Dazl-binding consensus motif (5′-$U_6GU_3GU_3GU_4$-3′) or a nonspecific mutant RNA molecule (5′-$A_6CA_3CA_3CA_4$-3′) were immobilized on a NeutrAvidin-coated sensor chip. Dazl-RRM-WT or S65D proteins were flowed over the chip as analytes, and binding affinities were determined. The results demonstrate that although neither protein binds to the nonspecific RNA, both the wild-type RRM and the S65D mutant RRM bind to the RNA consisting of the Dazl-binding consensus sequence (Figure 3A). Furthermore, determination of the dissociation constant (K_D) similarly revealed no significant difference in the association of either protein with the Dazl-binding RNA consensus sequence (Figure 3B and Supplemental Figure S2). These findings are consistent with the crystal structure of the murine Dazl RRM, which was solved in complex with three different target RNAs (Jenkins *et al.*, 2011) and in which it is demonstrated that S65 does not make direct contact with the RNA molecule. These results therefore suggest that posttranslational modification of this residue may regulate an alternative function of Dazl.

In response to heat stress in germ cells, Dazl localizes to stress granules (Kim *et al.*, 2012)—nonmembranous cytoplasmic foci composed of stalled translational complexes and associated RNA-binding proteins. In the absence of Dazl, stress granules do not form, and germ cells are more susceptible to stress-induced apoptosis (Kim *et al.*, 2012). We therefore tested whether mutation of S65 affects localization of Dazl to stress granules in response to arsenite treatment (Supplemental Figure S3). The results demonstrate that both wild-type and mutant forms of Dazl localize to stress granules, suggesting that modification of this residue is likewise not involved in mediating localization to these structures.

Once bound to the 3′ UTR of target mRNAs, Dazl functions as a translational enhancer by recruiting poly(A)-binding protein (PABP) to stimulate the initiation of translation (Collier *et al.*, 2005; Brook *et al.*, 2009). We therefore postulated that phosphorylation of S65 may affect translation by altering the association of Dazl with PABP,

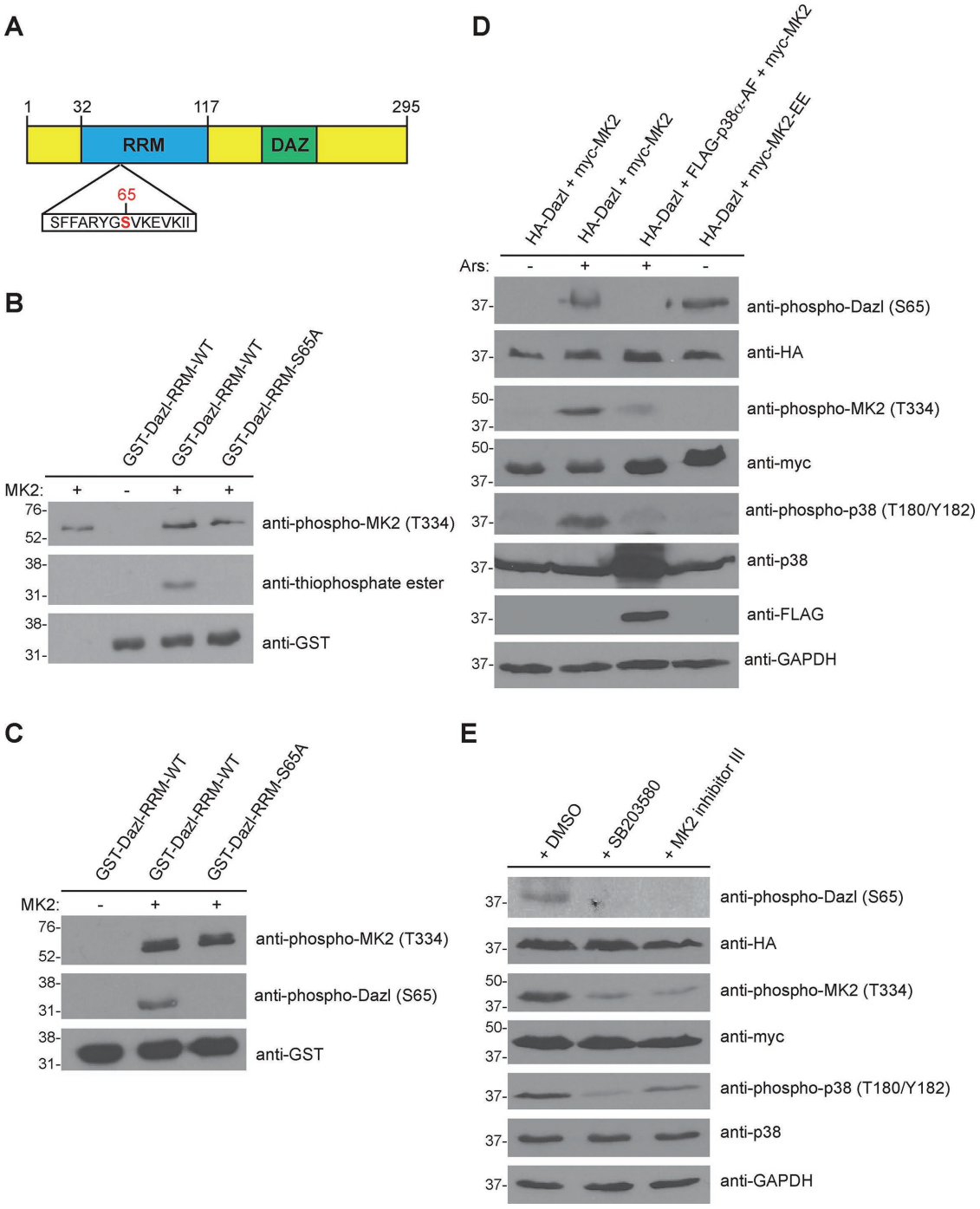

FIGURE 2: MK2 phosphorylates Dazl at S65. (A) Domain architecture of human Dazl. DAZ, deleted in azoospermia domain; RRM, RNA recognition motif. The putative MK2 phosphorylation site (S65) is indicated in red. (B) MK2-mediated phosphorylation of Dazl-S65 in vitro. Wild-type or S65A GST-Dazl-RRM (residues 32–117) fusion proteins were incubated with active recombinant MK2 and ATPγS, followed by incubation with PNBM. Kinase reactions were resolved by SDS–PAGE (on two separate gels), followed by immunoblotting with the indicated antibodies. (C) Detection of Dazl-S65 phosphorylation using a phosphospecific antibody. GST-Dazl RRM (wild-type or S65A) fusion proteins were incubated with active recombinant MK2 and ATP. Kinase reactions were resolved by SDS–PAGE (on two separate gels), followed by immunoblotting with the indicated antibodies. (D) Alteration of Dazl-S65 phosphorylation status via genetic manipulation of the p38-MK2 signaling pathway. HEK293 cells were transfected with the indicated constructs and either stimulated or not with sodium arsenite (Ars) and lysed. Cell lysates were split, resolved by SDS–PAGE (on eight separate gels), and immunoblotted with the indicated antibodies. Western blots shown are representative of three independent experiments. (E) Reduced Dazl-S65 phosphorylation by chemical inhibition of the p38-MK2 signaling pathway. HEK293 cells were transfected with the indicated constructs and pretreated for 30 min with DMSO (vehicle) only, the p38 inhibitor SB20350 (10 μM), or MK2 inhibitor III (20 μM). Cells were then stimulated with sodium arsenite and lysed. Cell lysates were split, resolved by SDS–PAGE (on seven separate gels), and immunoblotted with the indicated antibodies. Western blots shown are representative of three independent experiments.

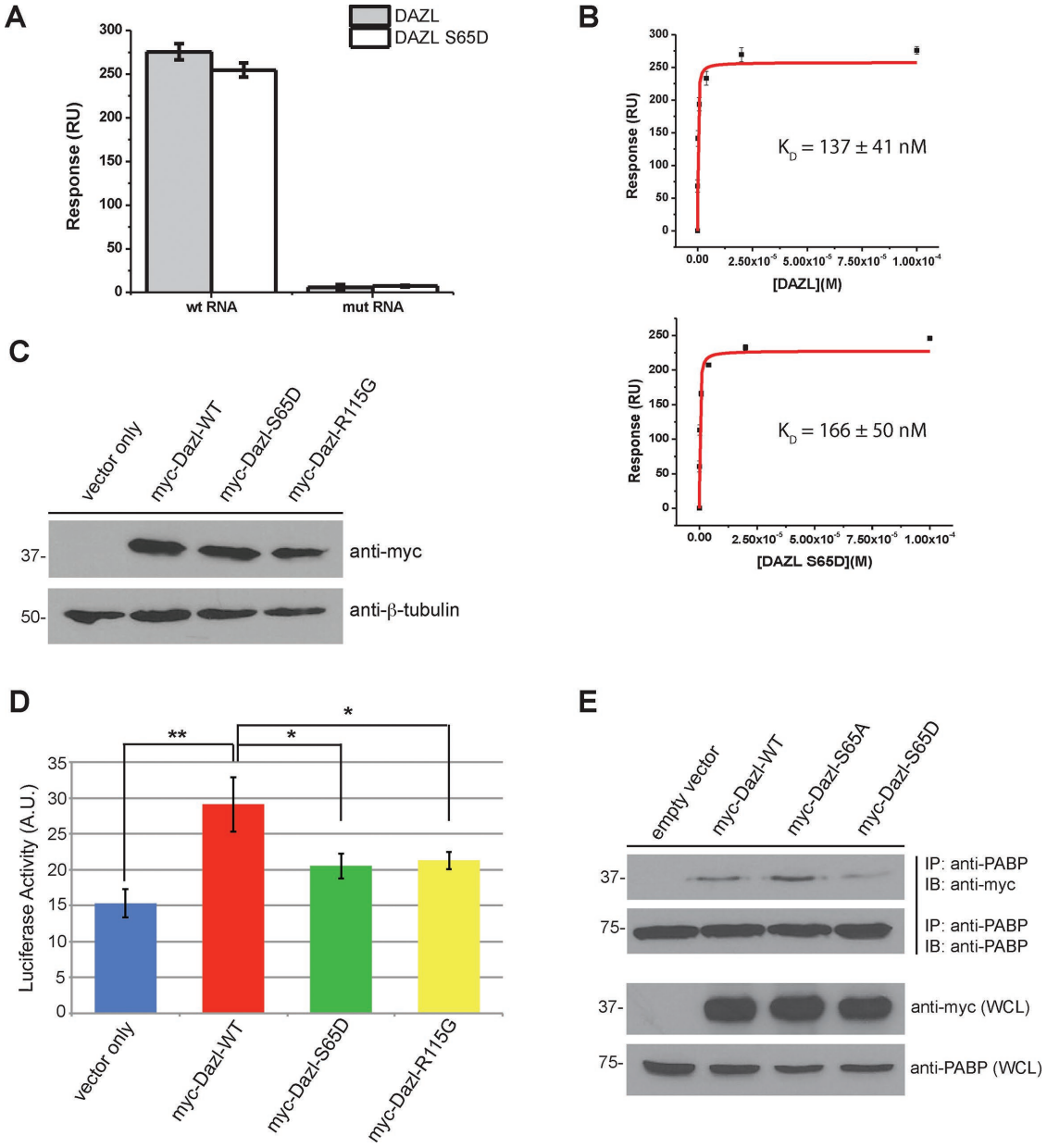

FIGURE 3: Mutation of Dazl S65 impairs translation but not RNA binding. (A) Bar chart depicting relative binding responses of wild-type and S65D Dazl-RRM proteins to wild-type and mutant (i.e., nonspecific control) RNAs. (B) Equilibrium binding plots of the interaction of wild-type and mutant Dazl-RRM proteins interacting with the wild-type RNA sequence. Data are representative of three independent experiments. Error bars represent one SD. (C) Expression of myc-tagged Dazl-WT, Dazl-S65D, and Dazl-R115G by immunoblotting of whole-cell lysates from transfected HeLa cells. (D) Reduced translation of a Dazl target upon expression of Dazl-S65D. HeLa cells were cotransfected with psiCHECK-2-SYCP3-3′UTR (a characterized Dazl-binding sequence cloned downstream of the sequence encoding *Renilla* luciferase) and the indicated Dazl constructs. Cells were lysed, and luciferase activity was quantified. Average of three independent experiments. Error bars indicate SD. *$p < 0.05$ and **$p < 0.005$ as calculated by a Student's *t* test. (E) Diminished binding of PABP to Dazl upon phosphomimetic mutation of S65. HEK293 cells were cotransfected with plasmids encoding PABP and pCMV-myc (empty vector), myc-Dazl-WT, myc-Dazl-S65A, or myc-Dazl-S65D. Cells were lysed, followed by immunoprecipitation of PABP and immunoblotting of the precipitated material with the indicated antibodies. Western blots shown are representative of three independent experiments. IB, immunoblot; IP, immunoprecipitate; WCL, whole-cell lysate.

and we addressed this possibility using a luciferase reporter assay. A plasmid was constructed in which the 3′ UTR of murine *SYCP3*, a validated Dazl-binding sequence (Reynolds *et al.*, 2007), was cloned downstream of the *Renilla* luciferase gene. HeLa cells were then transfected with this construct or cotransfected with this construct and a plasmid encoding myc-Dazl-WT, myc-Dazl-S65D, or, as a negative control, myc-Dazl-R115G, a mutant that is defective in RNA binding and is associated with human infertility (Tung *et al.*, 2006; Jenkins *et al.*, 2011). Western blotting was used to confirm equal expression of the myc-tagged proteins (Figure 3C), and luciferase

activity was measured to assay translation. The results demonstrate significantly less luciferase activity with expression of Dazl-R115G than with wild-type Dazl (Figure 3D). Moreover, cells expressing Dazl-S65D also displayed decreased luciferase activity (Figure 3D), suggesting that while mutation of this residue does not affect RNA binding, it does decrease translation. To determine whether this reduction in translation is due to inhibition of PABP binding, we cotransfected HEK293 cells with plasmids encoding untagged PABP and myc-Dazl-WT, myc-Dazl-S65D, myc-Dazl-S65A, or empty vector as a control. PABP was immunoprecipitated from cell lysates, and the immunoprecipitates were probed for Dazl (Figure 3E). Less Dazl-S65D coprecipitated with PABP than with Dazl-WT (and, reciprocally, less PABP coprecipitated with Dazl-S65D than with Dazl-WT; Supplemental Figure S4), whereas expression of Dazl-S65A appeared to stabilize the interaction (Figure 3E and Supplemental Figure S4). Taken together, these results suggest that MK2-mediated phosphorylation of Dazl decreases translation by inhibiting the interaction of Dazl with PABP.

Expression of human Dazl, but not Dazl-S65D, restores fertility in *boule* mutant flies

The *Drosophila* orthologue of Dazl is Boule, and *boule* mutant male flies are sterile due to a defect in meiotic entry (Eberhart *et al.*, 1996). Specifically, spermatocytes of *boule* mutants are arrested in meiosis I at the G2/M transition due to reduced translation of Twine (Maines and Wasserman, 1999), the meiotic Cdc25 phosphatase that dephosphorylates the cdc2/cyclinB complex. Overexpression of Twine in the *boule* mutant genetic background rescues this phenotype (Maines and Wasserman, 1999), as does transgenic expression of either human Boule (Xu *et al.*, 2003) or *Xenopus* Dazl (Houston *et al.*, 1998), illustrating the high degree of functional conservation among *DAZ* family members.

On the basis of these studies, we predicted that expression of human Dazl would rescue the *Drosophila boule* phenotype, whereas Dazl-S65D would not due to its reduced capacity to promote translation. To directly test this, we expressed myc-tagged human Dazl or Dazl-S65D in the male germline of *boule* mutants using the Gal4-*UAS* system. Western blotting of testis extracts demonstrated equal expression of the wild-type and mutant transgenes (Figure 4A). The fertility of male flies expressing these transgenes was assessed by a fertility assay. Expression of wild-type Dazl restored fertility in the *boule* mutant genetic background (Figure 4B), indicating that human Dazl can functionally compensate for the lack of *Drosophila* boule. Furthermore, analysis of testes by phase contrast microscopy revealed rescue of meiotic entry based on the presence of postmeiotic round spermatids and elongating sperm bundles in flies expressing wild-type Dazl (Figure 4C). In contrast, germ cells from flies expressing Dazl-S65D did not differentiate beyond the spermatocyte stage and phenotypically resembled *boule* mutants, demonstrating that the S65D mutation impairs the function of Dazl in vivo.

To determine whether the rescue of meiotic entry and restoration of fertility upon expression of wild-type Dazl correlated with restored expression of Twine, we analyzed levels of Twine protein in testes from flies of the aforementioned genotypes. Consistent with previous studies, we observed reduced levels of Twine in *boule* mutant testes that were restored upon expression of wild-type Dazl (Figure 4D). In contrast, expression of Dazl-S65D did not rescue Twine expression in the *boule* mutant genetic background (Figure 4D). Taken together, these results provide evidence that the phosphorylation status of Dazl-S65 regulates Twine translation, meiotic progression, and male fertility.

In summary, we found that phosphorylation of the RNA-binding protein Dazl by MK2 is a negative regulator of male meiosis (Figure 4E). Our data suggest that this is due to decreased recruitment of PABP, ultimately resulting in reduced translation of Dazl-regulated target RNAs. The precise molecular mechanism by which this occurs is unclear, although we speculate that it might involve a conformational change, since S65 of Dazl lies outside of the minimal region required for the PABP-Dazl interaction (Collier *et al.*, 2005).

An intriguing aspect of this work is the regulation of meiotic G2/M progression by MK2-mediated phosphorylation of Dazl. MK2 plays an important role in somatic cells in the mitotic G2/M checkpoint in response to DNA damage through direct phosphorylation of Cdc25 (Manke *et al.*, 2005). Our results indicate that MK2 plays a similar, albeit indirect, role in meiosis through phosphorylation of Dazl, arresting the meiotic cell cycle due to reduced translation of Twine.

The primary phenotype of MK2-knockout mice is increased resistance to lipopolysaccharide-induced endotoxic shock due to a dampened inflammatory response (Kotlyarov *et al.*, 1999). Our data suggest that in addition to being more resistant to inflammation, MK2-knockout male mice may also display an increased tolerance to heat-induced germ cell apoptosis. Although this remains to be tested, it opens up the possibility that MK2 kinase inhibitors may find utility in the treatment of male infertility.

MATERIALS AND METHODS

Antibodies and reagents

Anti-Dazl (E6), anti–c-Myc (9E10), anti-GST (Z-5), anti–β-tubulin (H-235), anti–glyceraldehyde-3-phosphate dehydrogenase (6C5), anti-Vasa (d-260), and anti-PABP (10E10) antibodies were from Santa Cruz Biotechnology (Dallas, TX). Anti-MK2, anti–phospho-MK2 (T222), anti–phospho-MK2 (T334), anti-p38, anti–phospho-p38 (T180/Y182), anti-Hsp27, and anti–phospho-Hsp27 (S82) antibodies were from Cell Signaling Technology (Danvers, MA). Anti-HA antibody (16B12) was from Covance (Princeton, NJ). Anti–thiophosphate ester antibody (51-8) and *p*-nitrobenzyl mesylate (PNBM) were from Abcam (Cambridge, MA). ATP, ATPγS, 4′,6-diamidino-2-phenylindole, and sodium arsenite were from Sigma-Aldrich (St. Louis, MO). The p38 MAPK inhibitor SB203580 was from Selleckchem (Houston, TX), and MK2 inhibitor III was from Cayman Chemical (Ann Arbor, MI).

Cell culture

HEK293 and HeLa cells were grown in DMEM supplemented with 10% fetal bovine serum (FBS) and penicillin/streptomycin. SUM149 cells were grown in Ham's F12 medium supplemented with 5% FBS, penicillin/streptomycin, insulin (5 μg/ml), and hydrocortisone (1 μg/ml). Cells were grown at 37°C in 5% CO_2. Lipofectamine 2000 (Invitrogen, Carlsbad, CA) was used for transfection according to the manufacturer's instructions. To induce oxidative stress, cells were stimulated with 0.5 mM sodium arsenite for 20 min at 37°C. To prepare lysates for immunoblotting or immunoprecipitation, cells were lysed by scraping in ice-cold lysis buffer (20 mM Tris, pH 8.0, 200 mM NaCl, and 1% Triton X-100 with protease inhibitors [Roche, Indianapolis, IN] and phosphatase inhibitors [1 mM sodium orthovanadate, 10 mM sodium fluoride, and 1 mM β-glycerophosphate]).

Generation of MK2-knockdown cell line

Retroviral shRNA constructs targeting human MK2 and a scrambled control shRNA construct were purchased from OriGene (Rockville, MD). Stably transfected SUM149 cells were selected with puromycin

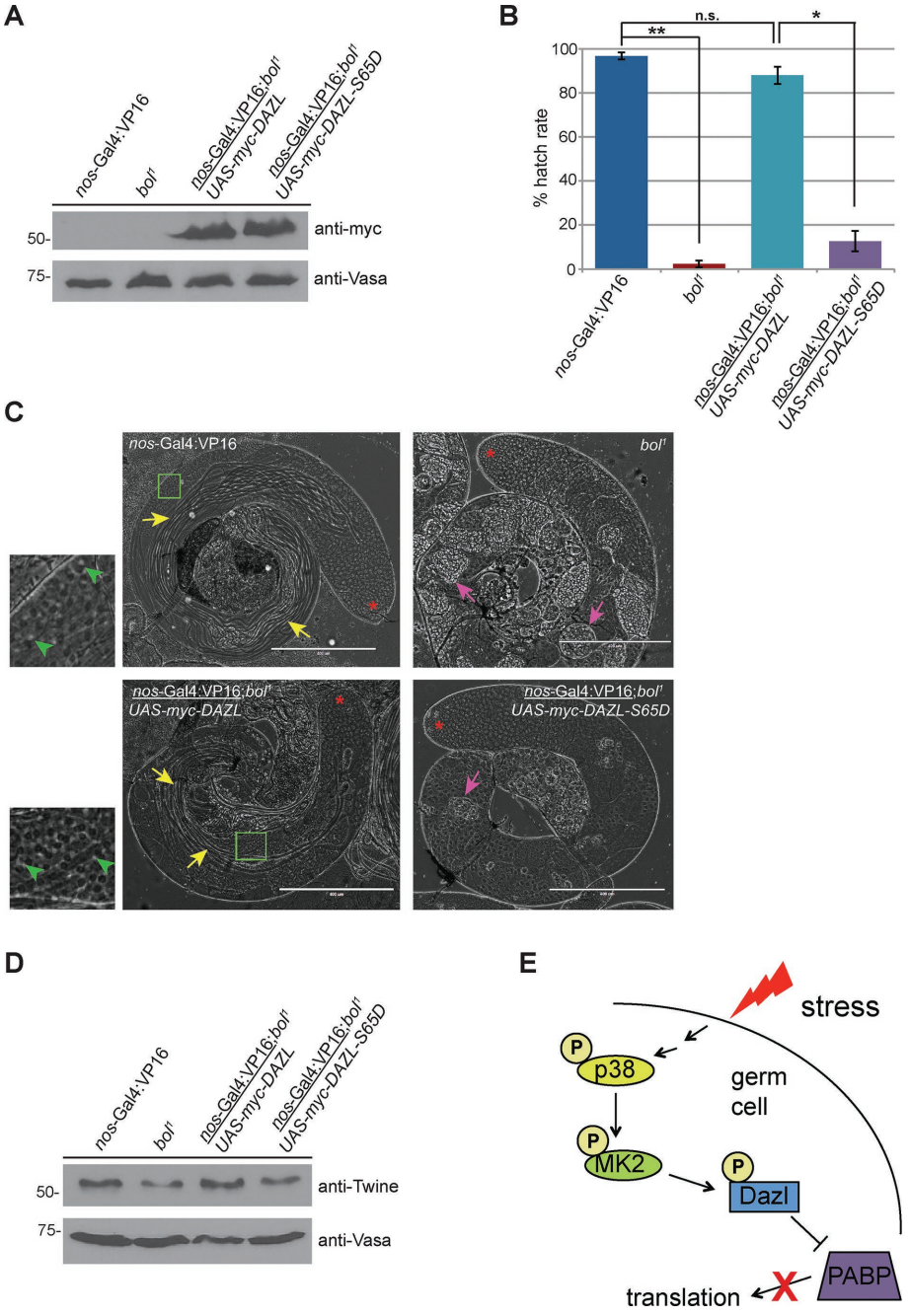

FIGURE 4: Expression of Dazl, but not Dazl-S65D, rescues meiotic defects and infertility in *boule* mutant male flies. (A) Expression of human myc-tagged Dazl or Dazl-S65D in the *Drosophila* male germline. Testes from flies of the indicated genotypes were dissected, and protein extracts were resolved by SDS–PAGE and immunoblotted with the indicated antibodies. (B) Transgenic expression of wild-type human Dazl in the *Drosophila* male germline rescues the sterility of *boule* mutants. Hatch-rate analysis from crosses of male flies of the indicated genotype to w^{1118} virgin females. Mean values from three independent experiments. Error bars denote SD. *$p < 0.05$ and **$p < 0.005$ as calculated by a Student's *t* test. n.s., not significant. (C) Phase contrast microscopy of live testes from flies of the indicated genotypes. Yellow arrows denote bundles of elongating spermatids that are absent in testes of bol^1 flies and flies expressing the human *DAZL-S65D* transgene in the bol^1 genetic background. Green boxes denote areas displayed in magnified insets. Green arrowheads indicate examples of round ("onion-stage") spermatids characterized by a phase-light nucleus juxtaposed to a phase-dark mitochondrial aggregate. Pink arrows indicate cysts of degenerating primary spermatocytes. Red asterisks denote the apical end of the testis. Scale bar, 400 µm. (D) Expression of twine in testes from flies of the indicated genotypes. Testes were dissected, and protein extracts were resolved by SDS–PAGE, followed by immunoblotting with the indicated antibodies. Western blots shown are representative of three independent experiments. (E) Model. Cellular stress induces phosphorylation of Dazl S65 via the p38-MK2 kinase pathway in male germ cells. This posttranslational modification decreases the binding of Dazl to PABP, leading to reduced translation of the proteins encoded by those mRNAs.

(1 µg/ml) were maintained in medium containing puromycin (0.5 µg/ml). Knockdown of MK2 was confirmed by Western blotting.

Plasmids

Human MK2 was PCR amplified as an *Eco*RI–*Not*I fragment from a cDNA clone (OriGene) and cloned into the corresponding sites of pCMV-myc (Clontech, Mountain View, CA). A plasmid encoding dominant-negative p38 (FLAG-p38 alpha [AF]) was provided by Roger Davis (University of Massachusetts Medical School, Worcester, MA; plasmid #20352; Addgene). A construct encoding constitutively active MK2 (pCDNA3-myc-MK2-EE) was provided by Matthias Gaestel (Hannover Medical School, Germany). A plasmid encoding human PABP was purchased from OriGene. Human Dazl was PCR amplified from a cDNA clone (OriGene) as an *Eco*RI–*Bgl*II fragment and cloned into the corresponding sites of pCMV-myc (Clontech) and pCMV-HA (Clontech). The S65A, S65D, and R115G mutations were introduced by PCR-mediated site-directed mutagenesis using the QuikChange Kit (Agilent, Wilmington, DE). For bacterial expression of GST-tagged Dazl-RRM fusion proteins, residues 32–117 of Dazl were PCR amplified as *Bam*HI–*Eco*RI fragments and cloned into the corresponding sites of pGEX-6P-1 (GE Healthcare, Chicago, IL). Oligonucleotides were purchased from Integrated DNA Technologies (Coralville, IA). Primer sequences are available upon request. All constructs were fully sequenced.

Protein microarrays and data analysis

The Snapshot Proteomics screen was conducted by AVMBioMed (Malvern, PA). Protein microarrays (consisting of >20,000 human proteins) were blocked for 1 h at room temperature in phosphate-buffered saline (PBS) containing 0.05% Tween-20, 20 mM reduced glutathione, 1 mM dithiothreitol (DTT), 1% bovine serum albumin, and 25% glycerol. Duplicate arrays were incubated for 90 min at room temperature using the two cell lysates (control shRNA and MK2 shRNA) at 2 mg/ml total protein concentration, followed by three washes with 1× PBS. Arrays were then incubated for 1 h at room temperature with rabbit anti–phosphoserine (Cell Signaling Technology) and rabbit

anti–phosphothreonine (Abcam) antibodies per the manufacturer's instructions for immunoblotting. Arrays were washed three more times, followed by a 1-h incubation with Alexa 488-conjugated anti-rabbit secondary antibody. This was followed by two washes with PBS/Tween-20, PBS, and then two washes with water, followed by centrifugal drying (1000 rpm for 5 min at room temperature) and scanning (GenePix 4100A; Molecular Devices) of the arrays.

Data were obtained from 21,685 proteins present on the microarray. Microarray images were gridded and quantitated using GenePix Pro (version 7) software. Median intensities (features and local backgrounds) were used, and signal-to-noise ratio (SNR) was calculated. Duplicate features representing identical proteins were summarized by average (avg *M*) and SD. Magnitude change was calculated as $\log(SNR)^{\text{control shRNA}} - \log(SNR)^{\text{MK2 shRNA}}$. These values were then Loess transformed by print tip and location to remove technical sources of error (Smyth and Speed, 2003), resulting in the final estimate of magnitude change (*M* value). To assess statistical significance, a paired, two-tailed Student's *t* test was used to calculate a *p* value for each estimate using the null hypothesis that avg $M = 0$. A threshold of 95% confidence ($p < 0.05$) and a cutoff of $M > 1.0$ were applied to filter the data.

Fly stocks and transgenic fly lines

Stocks were maintained and all crosses performed at 25°C on molasses-based food. *bol*^{1} flies were kindly provided by Steve Wasserman (University of California, San Diego, La Jolla, CA). Human *DAZL* or *DAZL-S65D* was PCR amplified using *attB*-modified primers and cloned into pDONR-Zeo (Invitrogen). The cloned inserts were transferred into pTMW using Gateway cloning technology to create N-terminal myc-tagged constructs for *Drosophila* embryo microinjection. Transgenic flies were generated by BestGene (Chino Hills, CA). *UAS-DAZL* maps to the third chromosome, and *UAS-DAZL-S65D* maps to the second chromosome.

Protein expression and purification

BL21(DE3) cells (Novagen, Billerica, MA) were transformed with plasmids encoding GST, GST-Dazl, GST-Dazl-S65A, GST-Dazl-RRM-WT, GST-Dazl-RRM-S65D, or GST-Dazl-RRM-R115G. Protein expression was induced at 37°C for 2 h with 1 mM isopropyl-β-D-thiogalactoside (IPTG). After centrifugation, the pellet was resuspended in 15 ml of lysis buffer (20 mM Tris, pH 7.4, 150 mM NaCl, 1 mM DTT, and 1 mM EDTA with protease inhibitors [Roche]). The lysate was sonicated on ice and centrifuged at 20,000 × *g* for 20 min at 4°C. The supernatant was added to 0.5 ml (packed volume) of glutathione agarose beads (Gold Biotechnology, St. Louis, MO) and incubated at 4°C for 2 h with end-over-end tumbling. The slurry was transferred to a column and washed extensively with wash buffer. GST-fusion proteins were eluted with excess glutathione in lysis buffer (pH 7.4), and appropriate fractions were pooled. The protein was dialyzed overnight at 4°C into dialysis buffer (20 mM Tris, pH 7.4, 150 mM NaCl, 1 mM DTT). Glycerol was added to a final concentration of 10%, and the proteins were snap-frozen and stored at –80°C.

In vitro kinase assays

Recombinant GST-tagged MK2 (residues 40–400; R&D Systems, Minneapolis, MN) was incubated with 20 μg of recombinant purified Dazl protein in kinase buffer (50 mM HEPES, pH 7.5, 0.65 mM $MgCl_2$, 0.65 mM $MnCl_2$, 12.5 mM NaCl) with 500 μM ATP or ATPγS, as indicated. Kinase reactions were incubated at 30°C for 30 min. When appropriate, PNBM (dissolved in dimethyl sulfoxide [DMSO]) was added to a final concentration of 2.5 mM, and reactions were incubated at room temperature for 1 h, followed by the addition of 6× boiling sample buffer to stop the reaction. Reactions were then resolved by SDS–PAGE, followed by immunoblotting with the indicated antibodies.

Generation of anti–phospho-S65-dazl antibody

A custom phosphospecific antibody was generated by GenScript (Piscataway, NJ). New Zealand white rabbits were injected with a phosphopeptide (ARYGpSVKEVKIITDC) conjugated to KLH. Sera were tested for sensitivity and specificity by enzyme-linked immunosorbent assay. The antibody was affinity purified against the phosphorylated peptide and negatively adsorbed against the nonphosphorylated peptide.

SDS–PAGE and Western blotting

Proteins were resolved on 12.5% polyacrylamide gels and transferred to nitrocellulose membranes (GE Amersham) using the Pierce G2 Fast Blotter (Thermo Scientific, Waltham, MA). Membranes were blocked in 5% nonfat milk in Tris-buffered saline (TBS), followed by overnight incubation with the indicated primary antibody in the same buffer. Membranes were washed the next day in TBS plus 0.5% Tween (TBS-T), incubated for 1 h with the appropriate horseradish peroxidase–conjugated secondary antibody, washed again in TBS-T, and processed for signal detection using enhanced chemiluminescence (Santa Cruz Biotechnology). For detection of proteins from the same reaction/lysate that migrate at similar molecular weights (i.e., phosphorylated and nonphosphorylated forms of the same protein), samples were split and run on separate gels.

Surface plasmon resonance

For protein expression for use in SPR, all plasmid DNA constructs were transformed into BL21(DE3) cells (Life Technologies). Cells were grown in Terrific Broth (RPI, Mount Prospect, IL) at 37°C in 2- to 8-l volumes using a LEX bioreactor (Epiphyte, Toronto, Canada), induced using 100 μM IPTG (CellGro, Manassas, VA) at 15°C, and harvested 12 h later by centrifugation at 4000 × *g* for 20 min. Pellets were stored at –80°C until purification. Bacterial cell pellets from 2-l culture volumes were thawed in warm water and then resuspended using binding buffer (50 mM Tris, pH 8.0, 500 mM NaCl) plus a 3:1 ratio of B-PER:Y-PER (Thermo Fisher), DNase 1, lysozyme, and protease inhibitor P2714 (all from Sigma-Aldrich). Cells were sonicated (frequency 60% maximum, 30 s on/30 s off, 5-min sonication time), and total lysate was mixed with 1–2 ml of His-Link resin (Promega, Madison, WI) and then incubated with rocking for 1 h at 4°C. His-Link resin was cleaned in batch mode by extensive washing with cold binding buffer and transferred into gravity columns (Bio-Rad, Hercules, CA) for final washes (with wash buffer: binding buffer plus 10 mM imidazole, pH 8.0) and elution (with elution buffer: binding buffer plus 250 mM imidazole, pH 8.0, and 10% glycerol). Size exclusion chromatography for all proteins was accomplished using a Sephadex 200 column (GE Healthcare) on an NGC Chromatography System (Bio-Rad) using gel filtration buffer (binding buffer plus 5 mM β-mercaptoethanol and 1 mM EDTA). Fractions were analyzed by SDS–PAGE and pooled. If needed, protein was concentrated using Vivaspin-20 concentrators with a 5000–molecular weight cut-off (GE Healthcare).

Experiments were performed using the ProteOn XPR36 SPR array system (Bio-Rad). ProteOn GLC sensor chips were preconditioned with two short pulses each (10 s) of 50 mM NaOH, 100 mM HCl, and 0.5% SDS. Then the system was equilibrated with PBS-T buffer (20 mM Na phosphate, 150 mM NaCl, and 0.1% polysorbate 20, pH 7.4). Individual ligand flow channels were activated for 5 min

at 25°C with a mixture of 1-ethyl-3-(3-dimethylaminopropyl carbodiimide hydrochloride) (0.2 M) and sulfo-*N*-hydroxysuccinimide (0.05 M). Immediately after chip activation, NeutrAvidin (ThermoFisher) at a concentration of 100 µg/ml in 10 mM sodium acetate, pH 5.0, was injected across ligand flow channels for 5 min at a flow rate of 30 µl min^{-1}. Excess active ester groups on the sensor surface were capped by a 5-min injection of 1 M ethanolamine HCl (pH 8.5). This resulted in the coupling of NeutrAvidin at a density of 9000 response units (an arbitrary unit that corresponds to 1 pg/mm^2). The SD in the immobilization level from the six spots within each channel was <4%. Synthetic 3′ biotinylated RNA oligonucleotides (IDT) were then affinity captured and used as ligand for the Dazl-RRM protein–binding experiments.

Dazl-RRM proteins at the indicated concentrations in RNA-protein binding buffer (20 mM Tris, pH 7.5, 100 mM NaCl, 1 mM $MgCl_2$, 0.005% Tween) were injected over the control (no oligonucleotide) and oligonucleotide surfaces at a flow rate of 100 µl/min for a 2-min association phase, followed by a 4-min dissociation phase at 25°C using the "one-shot" functionality of the ProteOn (Bravman *et al.*, 2006). Specific regeneration of the surfaces between injections was not needed due to the nature of the interaction. Data were analyzed using ProteOn Manager Software, version 3.0 (Bio-Rad). The responses of a buffer injection and responses from the reference flow cell were subtracted to account for nonspecific binding. Data were subjected to equilibrium analysis, plotting the response at equilibrium versus concentration and fitting to a steady-state model to obtain the equilibrium dissociation constant (K_D).

Dual luciferase assay

The 3′ UTR of *SYCP3* was PCR amplified from mouse genomic DNA as an *Xho*I–*Not*I fragment and cloned into the corresponding sites of psiCHECK-2 (Promega). HeLa cells were seeded in a 96-well plate and grown overnight to ~65% confluence. Cells were cotransfected with plasmids encoding myc-tagged Dazl, Dazl-S65D, or Dazl-R115G and psiCHECK-2/*SYCP3-3′UTR* or transfected with just psiCHECK-2/*SYCP3-3′UTR* alone. The next day, cells were lysed according to the protocol described in the dual luciferase reporter assay kit (Promega). Cell lysates were transferred to wide-bottom 96-well plates that were read on a GLOMAX-96 microplate luminometer. Firefly luciferase values were normalized to *Renilla* luciferase values for each individual condition (performed in triplicate). These values were averaged, and the Dazl-S65D and Dazl-R115G values were normalized to the values obtained from Dazl-WT. Statistical analysis was performed using a Student's *t* test to obtain a *p* value.

Hatch-rate analysis

Two males of the indicated genotype were crossed to five virgin w^{1118} females for 2 d. Flies were then transferred to a collection cage attached to a grape juice agar plate for overnight collection of deposited eggs. The hatch rate was determined by dividing the number of hatched embryos after 24 h by the total number of embryos deposited at 14 h.

Testes dissection and microscopy

Testes from 1-d-old male flies were dissected in PBS and prepared for microscopy as described (Sitaram *et al.*, 2014). Live testes were imaged by phase contrast microscopy using an EVOS FL Auto microscope (Life Technologies) equipped with a 10× objective. For immunofluorescence microscopy using HeLa cells, cells were seeded on glass coverslips and transfected the next day with the indicated constructs for 24 h. Cells were then fixed in 4% formaldehyde and processed for immunofluorescence microscopy. Cells were imaged using an EVOS FL Auto microscope equipped with a 40× objective.

ACKNOWLEDGMENTS

We thank M. Gaestel, S. Wasserman, and P. O'Farrell for fly stocks and reagents and L. Steel for experimental advice. This work was supported by National Institutes of Health Grants R00GM094293 to T.L.D. and 1R56AI118415-01A1 to S.C. and start-up funds from Drexel University College of Medicine to T.I.S.

REFERENCES

Ben-Levy R, Leighton IA, Doza YN, Attwood P, Morrice N, Marshall CJ, Cohen P (1995). Identification of novel phosphorylation sites required for activation of MAPKAP kinase-2. EMBO J 14, 5920–5930.

Bravman T, Bronner V, Lavie K, Notcovich A, Papalia GA, Myszka DG (2006). Exploring "one-shot" kinetics and small molecule analysis using the ProteOn XPR36 array biosensor. Anal Biochem 358, 281–288.

Brook M, Smith JW, Gray NK (2009). The DAZL and PABP families: RNA-binding proteins with interrelated roles in translational control in oocytes. Reproduction 137, 595–617.

Collier B, Gorgoni B, Loveridge C, Cooke HJ, Gray NK (2005). The DAZL family proteins are PABP-binding proteins that regulate translation in germ cells. EMBO J 24, 2656–2666.

Dass B, Tardif S, Park JY, Tian B, Weitlauf HM, Hess RA, Carnes K, Griswold MD, Small CL, Macdonald CC (2007). Loss of polyadenylation protein tauCstF-64 causes spermatogenic defects and male infertility. Proc Natl Acad Sci USA 104, 20374–20379.

Eberhart CG, Maines JZ, Wasserman SA (1996). Meiotic cell cycle requirement for a fly homologue of human Deleted in Azoospermia. Nature 381, 783–785.

Gaestel M (2006). MAPKAP kinases—MKs—two's company, three's a crowd. Nat Rev Mol Cell Biol 7, 120–130.

Gutti RK, Tsai-Morris CH, Dufau ML (2008). Gonadotropin-regulated testicular helicase (DDX25), an essential regulator of spermatogenesis, prevents testicular germ cell apoptosis. J Biol Chem 283, 17055–17064.

Hecht N.B (1998). Molecular mechanisms of male germ cell differentiation. BioEssays 20, 555–561.

Houston DW, Zhang J, Maines JZ, Wasserman SA, King ML (1998). A Xenopus DAZ-like gene encodes an RNA component of germ plasm and is a functional homologue of Drosophila boule. Development 125, 171–180.

Hsu LC, Chen HY, Lin YW, Chu WC, Lin MJ, Yan YT, Yen PH (2008). DAZAP1, an hnRNP protein, is required for normal growth and spermatogenesis in mice. RNA 14, 1814–1822.

Idler RK, Yan W (2012). Control of messenger RNA fate by RNA-binding proteins: an emphasis on mammalian spermatogenesis. J Androl 33, 309–337.

Jenkins HT, Malkova B, Edwards TA (2011). Kinked beta-strands mediate high-affinity recognition of mRNA targets by the germ-cell regulator DAZL. Proc Natl Acad Sci USA 108, 18266–18271.

Jia Y, Castellanos J, Wang C, Sinha-Hikim I, Lue Y, Swerdloff RS, Sinha-Hikim AP (2009). Mitogen-activated protein kinase signaling in male germ cell apoptosis in the rat. Biol Reprod 80, 771–780.

Jiao X, Trifillis P, Kiledjian M (2002). Identification of target messenger RNA substrates for the murine deleted in azoospermia-like RNA-binding protein. Biol Reprod 66, 475–485.

Kim B, Cooke HJ, Rhee K (2012). DAZL is essential for stress granule formation implicated in germ cell survival upon heat stress. Development 139, 568–578.

Kotlyarov A, Neininger A, Schubert C, Eckert R, Birchmeier C, Volk HD, Gaestel M (1999). MAPKAP kinase 2 is essential for LPS-induced TNF-alpha biosynthesis. Nat Cell Biol 1, 94–97.

Maegawa S, Yamashita M, Yasuda K, Inoue K (2002). Zebrafish DAZ-like protein controls translation via the sequence "GUUC." Genes Cells 7, 971–984.

Mahtani KR, Brook M, Dean JL, Sully G, Saklatvala J, Clark AR (2001). Mitogen-activated protein kinase p38 controls the expression and post-translational modification of tristetraprolin, a regulator of tumor necrosis factor alpha mRNA stability. Mol Cell Biol 21, 6461–6469.

Maines JZ, Wasserman SA (1999). Post-transcriptional regulation of the meiotic Cdc25 protein Twine by the Dazl orthologue Boule. Nat Cell Biol 1, 171–174.

Manke IA, Nguyen A, Lim D, Stewart MQ, Elia AE, Yaffe MB (2005). MAPKAP kinase-2 is a cell cycle checkpoint kinase that regulates the G2/M transition and S phase progression in response to UV irradiation. Mol Cell 17, 37–48.
Paronetto MP, Sette C (2010). Role of RNA-binding proteins in mammalian spermatogenesis. Int J Androl 33, 2–12.
Reynolds N, Collier B, Bingham V, Gray NK, Cooke HJ (2007). Translation of the synaptonemal complex component Sycp3 is enhanced in vivo by the germ cell specific regulator Dazl. RNA 13, 974–981.
Reynolds N, Collier B, Maratou K, Bingham V, Speed RM, Taggart M, Semple CA, Gray NK, Cooke HJ (2005). Dazl binds in vivo to specific transcripts and can regulate the pre-meiotic translation of Mvh in germ cells. Hum Mol Genet 14, 3899–3909.
Reynolds N, Cooke HJ (2005). Role of the DAZ genes in male fertility. Reprod Biomed Online 10, 72–80.
Rockett JC, Mapp FL, Garges JB, Luft JC, Mori C, Dix DJ (2001). Effects of hyperthermia on spermatogenesis, apoptosis, gene expression, and fertility in adult male mice. Biol Reprod 65, 229–239.
Rousseau S, Morrice N, Peggie M, Campbell DG, Gaestel M, Cohen P (2002). Inhibition of SAPK2a/p38 prevents hnRNP A0 phosphorylation by MAPKAP-K2 and its interaction with cytokine mRNAs. EMBO J 21, 6505–6514.
Ruggiu M, Speed R, Taggart M, McKay SJ, Kilanowski F, Saunders P, Dorin J, Cooke HJ (1997). The mouse Dazla gene encodes a cytoplasmic protein essential for gametogenesis. Nature 389, 73–77.
Saunders PT, Turner JM, Ruggiu M, Taggart M, Burgoyne PS, Elliott D, Cooke HJ (2003). Absence of mDazl produces a final block on germ cell development at meiosis. Reproduction 126, 589–597.
Sitaram P, Hainline SG, Lee LA (2014). Cytological analysis of spermatogenesis: live and fixed preparations of Drosophila testes. J Vis Exp 83, e51058.
Smyth GK, Speed T (2003). Normalization of cDNA microarray data. Methods 31, 265–273.
Stokoe D, Campbell DG, Nakielny S, Hidaka H, Leevers SJ, Marshall C, Cohen P (1992). MAPKAP kinase-2; a novel protein kinase activated by mitogen-activated protein kinase. EMBO J 11, 3985–3994.
Stokoe D, Caudwell B, Cohen PT, Cohen P (1993). The substrate specificity and structure of mitogen-activated protein (MAP). kinase-activated protein kinase-2. Biochem J 296, 843–849.
Tung JY, Rosen MP, Nelson LM, Turek PJ, Witte JS, Cramer DW, Cedars MI, Reijo-Pera RA (2006). Novel missense mutations of the Deleted-in-AZoospermia-Like (DAZL) gene in infertile women and men. Reprod Biol Endocrinol 4, 40.
Vangompel MJ, Xu EY (2011). The roles of the DAZ family in spermatogenesis: more than just translation? Spermatogenesis 1, 36–46.
Venables JP, Cooke HJ (2000). Lessons from knockout and transgenic mice for infertility in men. J Endocrinol Invest 23, 584–591.
Venables JP, Ruggiu M, Cooke HJ (2001). The RNA-binding specificity of the mouse Dazl protein. Nucleic Acids Res 29, 2479–2483.
Winzen R, Kracht M, Ritter B, Wilhelm A, Chen CY, Shyu AB, Muller M, Gaestel M, Resch K, Holtmann H (1999). The p38 MAP kinase pathway signals for cytokine-induced mRNA stabilization via MAP kinase-activated protein kinase 2 and an AU-rich region-targeted mechanism. EMBO J 18, 4969–4980.
Wu X, Tian L, Li J, Zhang Y, Han V, Li Y, Xu X, Li H, Chen X, Chen J, *et al.* (2012). Investigation of receptor interacting protein (RIP3)-dependent protein phosphorylation by quantitative phosphoproteomics. Mol Cell Proteomics 11, 1640–1651.
Xu EY, Lee DF, Klebes A, Turek PJ, Kornberg TB, Reijo Pera RA (2003). Human BOULE gene rescues meiotic defects in infertile flies. Hum Mol Genet 12, 169–175.
Xu EY, Moore FL, Pera RA (2001). A gene family required for human germ cell development evolved from an ancient meiotic gene conserved in metazoans. Proc Natl Acad Sci USA 98, 7414–7419.
Yin Y, Hawkins KL, DeWolf WC, Morgentaler A (1997). Heat stress causes testicular germ cell apoptosis in adult mice. J Androl 18, 159–165.